J Mater Sci (2009) 44:3349–3355
DOI 10.1007/s10853-009-3408-9

The effect of NiO on the phase formation, thermo-physical properties and sealing behaviour of lithium zinc silicate glass–ceramics

Rakesh Kumar · A. Arvind · M. Goswami · S. Bhattacharya · V. K. Shrikhande · G. P. Kothiyal

Received: 10 November 2008 / Accepted: 16 March 2009 / Published online: 16 April 2009

Abstract We have prepared lithium zinc silicate (LZS) glasses of compositions (mol%) $17.83Li_2O$–$17.73ZnO$–$(53.52 - x)SiO_2$–$5.25Na_2O$–$1.25P_2O_5$–$4.31B_2O_3$–x-NiO, where $0.5 \leq x \leq 2.0$, by the melt quench technique. The effect of NiO on the phase formation, thermo-physical properties and sealing behaviour of LZS glass–ceramics was studied using X-Ray diffraction (XRD), thermo-mechanical analysis (TMA) and microhardness (MH) measurements. It is found that NiO incorporation leads to a change in the role of ZnO from network modifier to intermediate oxide. The intermediate network forming Zn^{2+} ions would find it more difficult to diffuse and initiate the transformation of $Li_3Zn_{0.5}SiO_4$ to Li_2ZnSiO_4. Thus $Li_3Zn_{0.5}SiO_4$ is formed instead of Li_2ZnSiO_4 on addition of 2 mol% NiO. Scanning electron microscopy (SEM) and energy dispersive analysis of X-rays (EDAX) measurements at the glass–ceramic-to-metal interface reveal a change in the microstructure commensurate with the changing role of ZnO. Addition of NiO favoured interdiffusion of species at the interface leading to better sealing.

Introduction

Glass–ceramics are a kind of polycrystalline materials formed by controlled crystallization of parent glasses. They offer a number of advantages compared to glasses such as tunable thermal expansion coefficient (TEC), enhanced mechanical properties and better tolerance to corrosive ambient. Glass–ceramics of the lithium zinc silicate (LZS) system are a versatile class of materials first reported by McMillan et al. [1] in the 1960s having application in hermetic sealing with various metals including stainless steels and Ni-based super alloys [2–5]. The predominant phases formed in this system are Li_2ZnSiO_4 and a variety of silica phases such as tridymite, quartz or cristobalite. The TEC of Li_2ZnSiO_4 is less than that of the silica phases. Therefore, a judicious optimization of the relative fractions of these phases can allow precise tailoring of the TEC of the glass–ceramics. The addition of group IV, V and VI transition metal oxides (TMOs) such as Ta_2O_5 or Nb_2O_5 to LZS glasses can reduce the fraction of high TEC silica phases and encourage the formation of lower TEC phases [6]. In this study, we aim to evaluate the effect of NiO addition on the thermo-physical properties and phase evolution in LZS glasses. Glass–ceramic-to-metal (GCM) seals are also fabricated and the interface studies using scanning electron microscopy (SEM) and energy dispersive analysis of X-rays (EDAX) are carried out in order to understand the sealing mechanism.

Experimental procedure

The compositions of LZS glasses prepared as part of this study are given in Table 1. They are referred to as LZSHNi-1 (0.5 mol% NiO), LZSHNi-2 (1.0 mol% NiO), LZSHNi-3 (1.5 mol% NiO) and LZSHNi-4 (2.0 mol% NiO). These glasses are synthesized by the melt quench technique as reported previously [7, 8]. In brief, analytical grade reagents SiO_2, Li_2CO_3, KNO_3, B_2O_3, ZnO, $(NH_4)_2HPO_4$ and NiO were used as starting materials. The batch was calcined in recrystallized alumina crucibles

R. Kumar · A. Arvind · M. Goswami · S. Bhattacharya · V. K. Shrikhande · G. P. Kothiyal (✉)
Technical Physics and Prototype Engineering Division, Bhabha Atomic Research Centre, Mumbai 400085, India
e-mail: gpkoth@barc.gov.in

Table 1 Compositions of LZSHNi glasses prepared

Sample	Composition in mol%						
	SiO_2	Li_2O	Na_2O	ZnO	B_2O_3	P_2O_5	NiO
LZSHNi-1	53.12	17.83	5.25	17.73	4.31	1.25	0.5
LZSHNi-2	52.62	17.83	5.25	17.73	4.31	1.25	1.0
LZSHNi-3	52.12	17.83	5.25	17.73	4.31	1.25	1.5
LZSHNi-4	51.62	17.83	5.25	17.73	4.31	1.25	2.0

according to a schedule determined by the decomposition temperatures of the precursors. In order to ensure complete decomposition of nitrates and carbonates into oxides, the batch was weighed before and after calcination to ascertain weight loss. The calcined batch was melted under air ambient at 1,450–1,500 °C in a Pt-10%Rh crucible in a raising lowering hearth electric furnace (Model OKAY M/s Bysakh and Co. Kolkata) and held for 1 h to ensure melt homogenization. The poured glass was immediately transferred to an annealing furnace set at about 450 °C and held for 2–4 h for annealing before cooling down to room temperature. The vitreous nature of the annealed glass was verified by X-Ray diffraction (XRD) (Sieffert XRD 3003 TT X-Ray Diffractometer with collimated Cu Kα radiation).

The DTA measurements on glass powders were performed on a Setaram 92-15 TG/DTA apparatus that was calibrated using the melting points of high purity indium and zinc for low temperatures and Al for higher temperature (~700 °C). Accuracy of the determination using Pt crucibles was verified by taking standard materials such as quartz and barium carbonate for high temperatures and potassium nitrate for low temperature. The non-isothermal experiments were performed by heating approx. 40 mg of the sample in Pt crucibles under protective ambient, using empty Pt crucible as reference. A heating rate of 10 K/min was employed in the range 25–1,000 °C. Samples were crystallized according to the DTA data as detailed in Table 2. XRD in the $20 \leq 2\theta \leq 80°$ range in steps of 0.5° was used to identify the crystalline phases formed. Phase identification was achieved by comparing the XRD patterns with JCPDS powder diffraction files.

Table 2 Heat treatment schedule for crystallization of various LZSHNi glasses

Sample	T_1 (°C)	Dwell (h)	T_2 (°C)	Dwell (h)
LZSHNi-1	630	2	705	2
LZSHNi-2	635	2	705	2
LZSHNi-3	630	2	705	2
LZSHNi-4	550	2	705	2

Density of all glasses and glass–ceramics were measured by using the Archimede's principle taking distilled water as the immersion fluid. All weights were measured on a single scale electronic balance with an accuracy of ±0.02 g. Glass/glass–ceramic samples in the form of flat circular discs of diameter 10 mm and thickness 2 mm were made flat by polishing for thermo-mechanical analysis (TMA, Model 92-12 M/s Setaram, France). TMA was employed to measure the TEC and the extrapolated starting glass transition temperature (T_g). The experiments were carried out in a precisely controlled furnace under flowing Ar ambient at a heating rate of 10 K/min. Sample expansion was measured using a hemispherical silica probe with the sample under compressive load of 5 g. The TEC value reported is in the range 30–450 °C with an accuracy of ±5% and values of T_g are accurate to ±2 °C. For each reported value of TEC and T_g, at least four samples were evaluated to ensure reproducibility. MH measurements were performed on mirror polished glass and glass–ceramic samples by a Vicker's MH tester (Model VMHT 30 M M/s Leica). For all the glasses studied, an indentation load of 50 g for 5 s was employed, while a load of 100 g for 5 s was used in the case of glass–ceramic samples. Vicker's MH number (VHN) was calculated by measuring the diagonal length of the indentation made in the sample by a square base pyramidal indenter [9, 10]. The VHN numbers reported are the averaged values for at least 10 indentations, the error reported being the standard deviation in the measurements.

The glass–ceramics studied were used to fabricate GCM seals with a cylindrical housing (25-mm ID × 40-mm L) of SS321, containing a central pin of the same material. The composition of SS321 is given in Table 3. Glass powder (approximately 6 g) was used for all the seals. During seal preparation, the glass powder, housing and pin were assembled on a graphite jig. This jig was then transferred to the sealing furnace where it was heated to the sealing temperature of 900–950 °C and held there for 45 min before cooling down to the higher crystallization temperature as determined by DTA. The sample was kept at this temperature for 60 min and then the temperature was reduced to the lower crystallization temperature. A dwell time of 60 min was provided at this temperature also. The seal was then annealed at 450 °C and was subsequently cooled to room temperature in the furnace. The

Table 3 Composition of SS321.[a] The major components are listed, the rest being Fe

Elements	C	Mn	P	S	Si	Cr	Ni	Ti
Wt%	0.08	2.00	0.045	0.03	1.00	18	10.5	5C

[a] www.azom.com/details.asp?ArticleID=967#_Composition

seals are assigned the following nomenclature: Seal-1(LZSHNi-1), Seal-2(LZSHNi-2), Seal-3(LZSHNi-3) and Seal-4(LZSHNi-4). Seals fabricated were tested for leak tightness on a helium leak detector. Seals were sectioned using a Buehler linear precision saw (Model: Isomet 4000) and then polished to 1-μm surface finish and coated with a conductive film of Au for SEM/EDAX investigations. SEM (Vega MV2300T/40) was used to examine the microstructure at the GCM interface. EDAX was employed to discern interdiffusion of species across the interface.

Results

All the prepared compositions yield clear and transparent glass. Powder XRD patterns of all the glasses prepared show the characteristic broad peak of amorphous materials. DTA curves of LZSHNi-1 to 4 glasses are given in Fig. 1. The results of DTA measurements are summarized in Table 4. All the glasses show a T_g in the neighborhood of 440 °C. The DTA curves also display two exothermic peaks. The lower temperature peak probably corresponds to the formation of $LiZnSiO_4$ phase, while the higher temperature peak augurs the crystallization of a silica polymorph [11]. It is interesting to note that when concentration of NiO increases to 2 mol%, the broad DTA exotherm at around 630 °C migrates to the neighborhood of 550 °C. The width of this exotherm also reduces. At the same time, the higher temperature (~700 °C) exotherm remains unchanged with increasing NiO fraction. The values of T_g, first crystallization peak temperature (T_{p1}) and second crystallization peak temperature (T_{p2}) as a function of NiO fraction are listed in Table 4. The variations in density and thermo-mechanical properties of the parent glasses are given in Table 5. Parent glasses were crystallized to yield glass–ceramics by controlled heat treatment as mentioned in Table 2. The XRD patterns of the glass–ceramics are given in Fig. 2. As NiO fraction increases, reflections corresponding to Li_2ZnSiO_4 (PDF 24-0679) and cristobalite (PDF 76-0941) reduce in intensity, while the peaks corresponding to $Li_3Zn_{0.5}SiO_4$ (PDF 24-0685) become more intense. The resulting variation in thermo-mechanical properties of the glass–ceramics is given in Table 6. The DTA experiments were carried out on glass powder while glass discs were used for TMA. The difference in the nature of the sample accounts for the lower T_g values found in DTA compared to TMA.

The SEM micrographs of the GCM seal interface are shown in Fig. 3. In Seal-1 (Fig. 3a), the microstructure at the interface is made up of a number of densely interlocking dendritic grains of size 10–15 μm. In addition, a number of

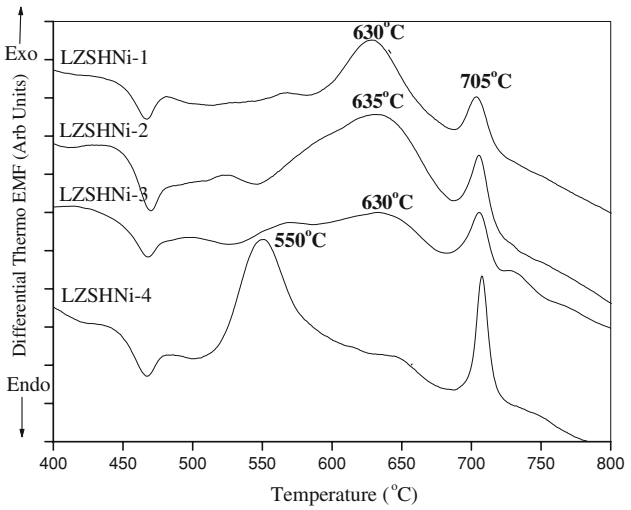

Fig. 1 DTA curves of LZSHNi samples at 10 K min^{-1}

Table 4 T_g and peak crystallization temperatures (T_{p1} & T_{p2}) from DTA for various LZSHNi glasses

Sample	T_g (°C) ± 2 °C	T_{p1} (°C) ± 2 °C	T_{p2} (°C) ± 2 °C
LZSHNi-1	440	630	705
LZSHNi-2	425	635	705
LZSHNi-3	438	630	705
LZSHNi-4	441	550	705

Table 5 Thermo-physical properties of LZSHNi glasses

Sample no.	Density (g/cc)	T_g (°C) ± 2 °C	μH (GPa)	TEC ($\times 10^{-6}$/°C) ± 5%
LZSHNi-1	2.85 ± 0.02	453	6.51 ± 0.01	12.5
LZSHNi-2	2.81 ± 0.03	457	6.63 ± 0.04	10.7
LZSHNi-3	2.86 ± 0.03	457	6.59 ± 0.03	9.7
LZSHNi-4	2.83 ± 0.04	451	6.55 ± 0.01	9.9

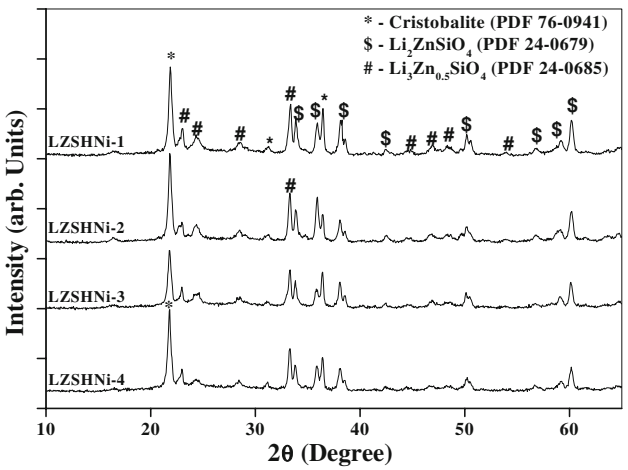

Fig. 2 XRD patterns of various LZSHNi glass–ceramics

Table 6 Thermo-physical properties of LZSHNi glass–ceramics. The errors in MH and density are standard deviations from mean

Sample no.	Density (g/cc)	T_g (°C) ± 2°C	μH (GPa)	TEC ($\times 10^{-6}$/°C) ± 5%
LZSHNi-1	2.79 ± 0.04	507	6.51 ± 0.03	16.3
LZSHNi-2	2.82 ± 0.02	507	6.55 ± 0.04	16.2
LZSHNi-3	2.86 ± 0.02	506	6.43 ± 0.02	15.4
LZSHNi-4	2.82 ± 0.03	504	6.34 ± 0.03	18.0

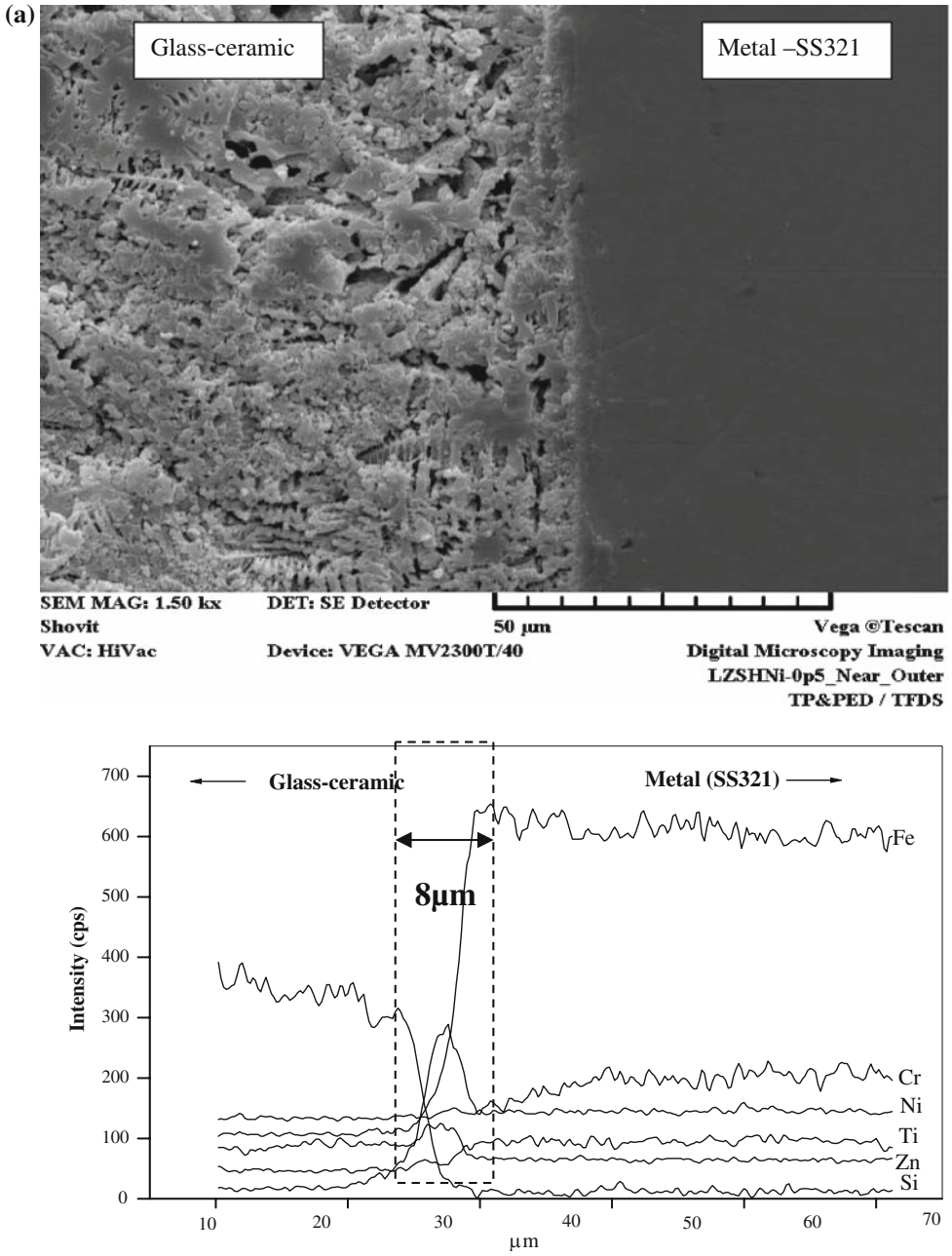

Fig. 3 The SEM micrograph of glass–ceramic to metal (GCM) seal interface of **a** Seal-1, **b** Seal-2 and **c** Seal-4, with respective EDAX line scans appended below

smaller aggregates of size 5–10 μm are also discernible. In case of Seal-2 (Fig 3b), the change in the interfacial microstructure is profound. The microstructure is composed of a few dendrites (5–10 μm) and a large number of irregularly shaped plate-like grains approximately 10–15 μm length and 5–10 μm width. The microstructure of Seal-4 is shown in Fig 3c. We observe that the microstructure is composed of long dendrites of length ~50 μm. These grow omni directionally and are less interlocked compared to the cases discussed above. In each of the seals described above, the

Fig. 3 continued

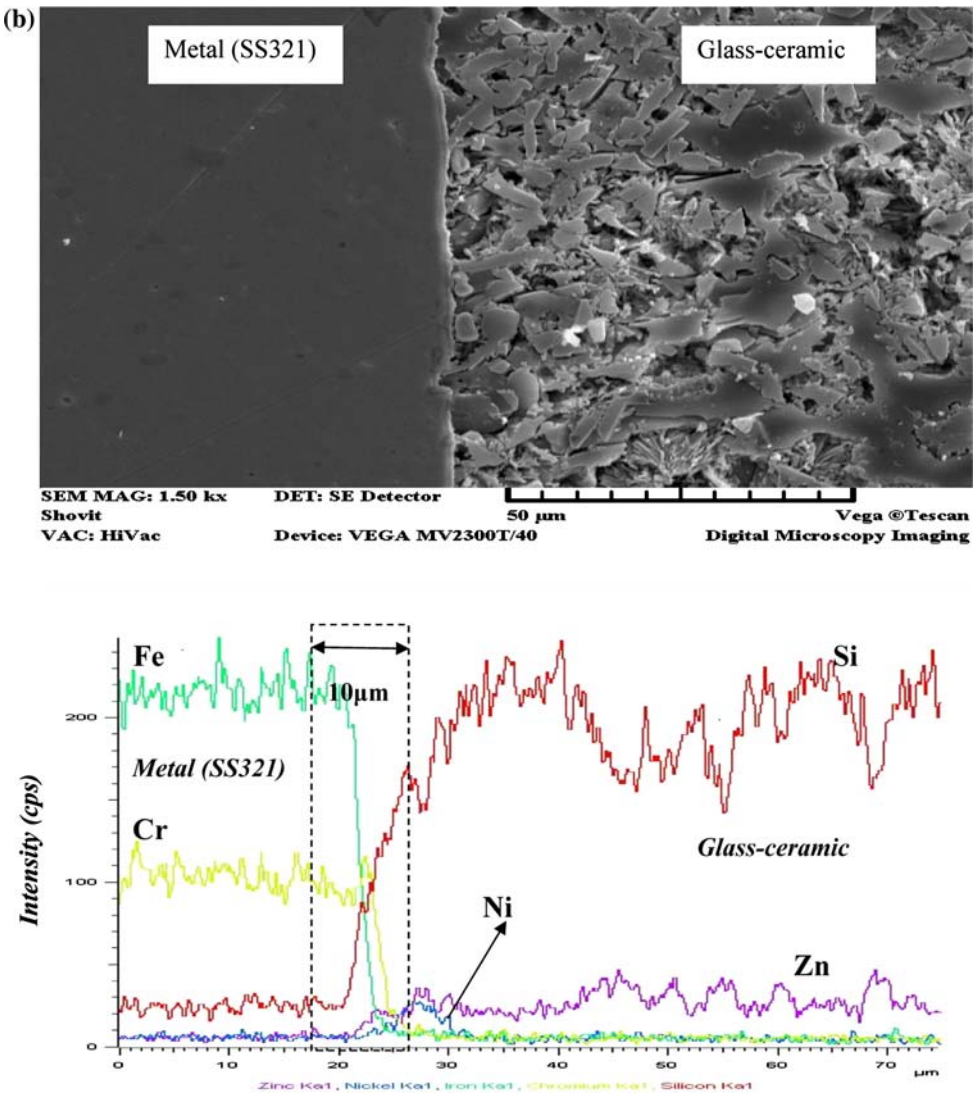

respective EDAX linescan is shown below each figure. We observe an interdiffusion of Si from the glass–ceramic into the metal to a depth of approximately 5–10 µm. EDAX also showed enrichment of Cr in proximity of the GCM interface. The interface also showed the formation of a layer enriched in Ni. The EDAX spot analysis carried out proximitous to the interface is shown in Fig 4. EDAX analysis on the particles near the interface confirms that these are enriched in Ni compared to other regions. Leak tests were performed on all the seals. They showed similar helium leak rates of less than 1.33×10^{-10} Pa m^3/s at a vacuum of 1.33×10^{-4} Pa.

Discussion

In parent glasses, on addition of NiO, the increase in MH with a commensurate decrease in the TEC does not agree well with the behaviour expected considering Ni^{2+} to be a network modifying cation [12]. It is known that Ni^{2+} ion has field strength higher than Zn^{2+}. Therefore, we believe that on incorporation of NiO, a greater number of O^{2-} ions are coordinated with the Ni^{2+} ion, thereby reducing the average oxygen coordination number about Zn^{2+}. It is documented in the literature that as the coordination number about Zn^{2+} reduces from 4 to 2, the role of ZnO changes from network modifier to intermediate oxide [13]. Therefore, on addition of NiO, an increasing fraction of Zn^{2+} ions assume the role of intermediate network formers. As a result of this, MH increases slightly while TEC reduces. The effect of NiO addition is also evident in DTA plots of the various LZS glasses. Out of the two observed exotherms, the first is progressively shifted to lower temperatures. The lower temperature exotherm corresponds to the formation of LZS phase, while the higher temperature one augurs the crystallization of a silica polymorph [6]. However, the exotherm corresponding to the formation of

Fig. 3 continued

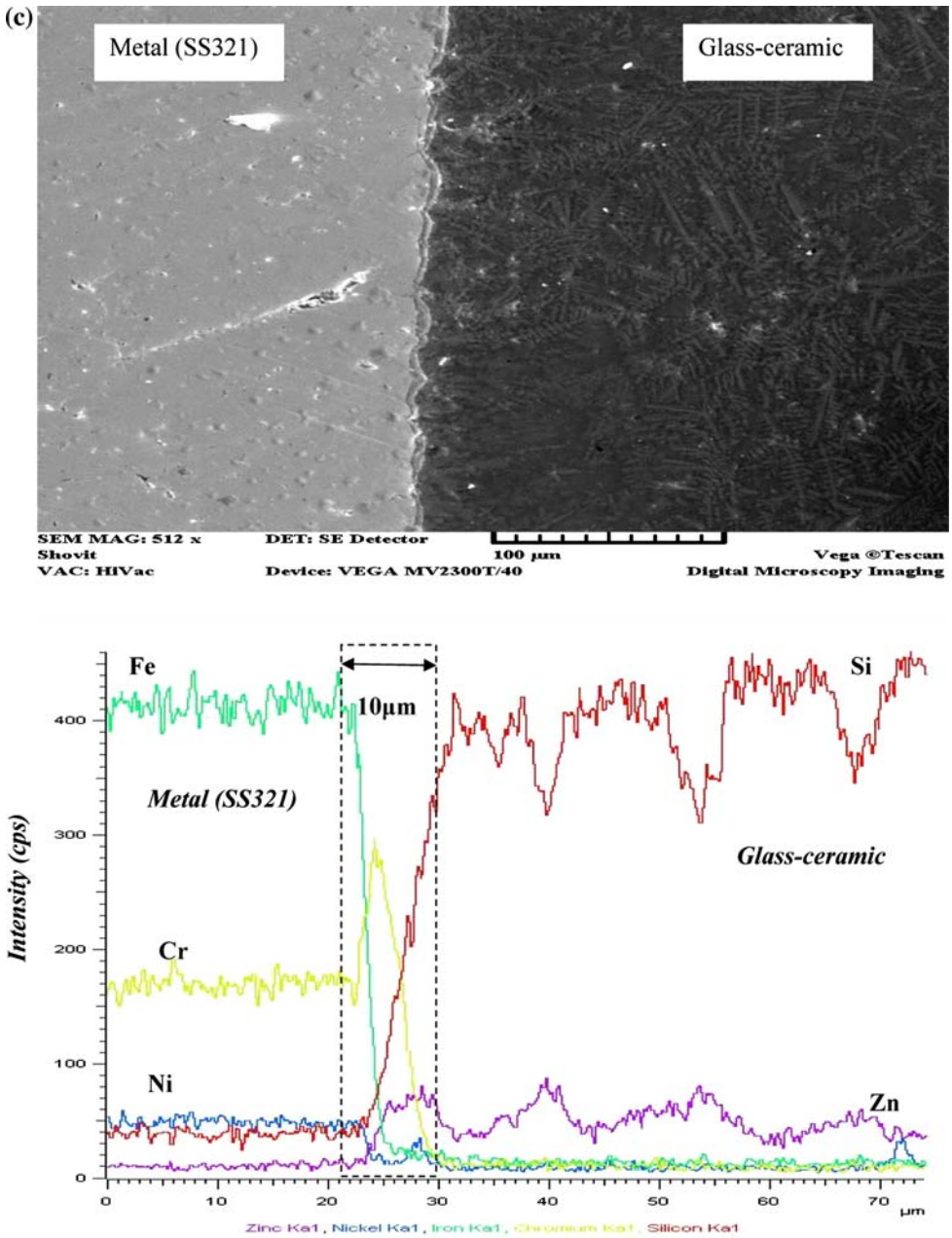

SiO_2 phase shows no positional dependence on NiO fraction [14, 15]. Not only does NiO addition encourage the formation of LZS, the composition of the phase also changes from Li_2ZnSiO_4 to $Li_3Zn_{0.5}SiO_4$. These findings agree well with previous study on LZS glasses, which reports the formation of two exothermic peaks in DTA/DSC [15].

As the role of ZnO changes, the average mobility of Zn^{2+} ions are expected to decrease encouraging the formation of $Li_3Zn_{0.5}SiO_4$ instead of Li_2ZnSiO_4 in LZSHNi-4. This occurs because intermediate network forming Zn^{2+} ions would find it more difficult to diffuse (lower mobility) and initiate the transformation of $Li_3Zn_{0.5}SiO_4$ to Li_2ZnSiO_4. In addition, a number of other factors such as viscosity, ion size and the local environment changes about the Zn^{2+} ions may also play a role. Up to 1.5% NiO fraction, Li_2ZnSiO_4 is one of the dominant phases. This phase has a comparatively high TEC [16] as a result of which, all the LZS glass–ceramics up to LZSHNi-3 have nearly the same TEC within experimental error. In case of LZSHNi-4, $Li_3Zn_{0.5}SiO_4$ is one of the phases formed instead of Li_2ZnSiO_4. The crystallization of this phase causes an increase in TEC and a marginal reduction in MH in this sample.

The addition of NiO also improves the sealing properties of the LZSH glass–ceramics. It is well known that for the formation of a seal, the glass at the interface must be

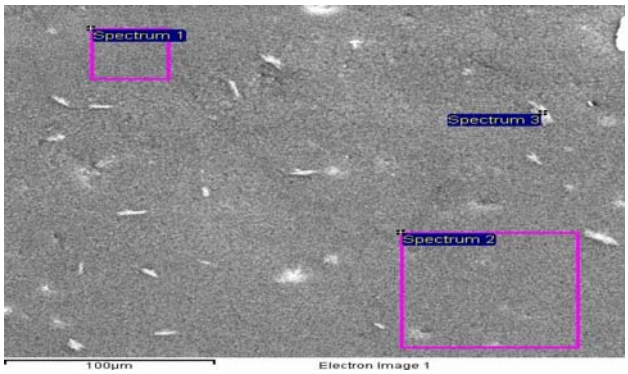

Spectrum	In stats.	O	Na	Si	Ni	Zn
		(Atomic %)				
Spectrum 1	Yes	47.67	7.48	33.22	0.95	10.68
Spectrum 2	Yes	46.86	7.49	32.82	0.92	11.90
Spectrum 3	Yes	45.59	3.76	32.91	9.24	8.51
Mean		46.71	6.24	32.98	3.70	10.36
Std. deviation		1.05	2.15	0.21	4.79	1.72
Max.		47.67	7.49	33.22	9.24	11.90
Min.		45.59	3.76	32.82	0.92	8.51

Fig. 4 Spot analysis of glass–ceramic near the interface showing the relative amounts of various species, which are tabulated below. Note the increased Ni concentration in Spectrum 3

saturated in the ions of the metal [17]. The presence of NiO in the glass seems to have helped the diffusion of ions from the glass–ceramic to the metal and vice versa. The SEM of the seals clearly shows the formation of an interfacial layer (Fig 3c). In the interfacial region, there probably exist small Ni rich particles dispersed along the interface and within the glass–ceramic in the proximity of the interface. This is evidenced by the Ni-enriched region close to the interface in EDAX. Therefore, in addition to changing the crystallization kinetics in the LZSH glass–ceramics, NiO acts as an adherence promoter [17].

It may react with Cr to yield Cr_2O_3 and Ni according to the reaction given below:

$$3NiO + 2Cr \rightarrow Cr_2O_3 + 3Ni$$

This could also explain the relative enrichment of Cr at the interface. It has been reported that NiO addition prevents depletion of nucleating agent (P_2O_5) from the interfacial region [5, 17]. Thus, addition of NiO mitigates the formation of cristobalite, while improving the performance of LZSH glass–ceramic as a sealant to SS 321. In a previous study reporting on the sealing of SS321 using LZS glass–ceramics without NiO, it was observed that seal formation was not possible according to the cooling cycle employed here [7]. Goswami et al. [7] had established that the cooling cycle resulted in surface crystallization. By addition of NiO, we are able to achieve bulk crystallization in LZSH glass–ceramics using the cooling cycle and achieve a good hermetic seal.

Conclusion

The addition of NiO modified the crystallization behaviour of LZS glasses by mitigating the formation of cristobalite. Up to 1.5 mol% NiO addition, Li_2ZnSiO_4 was one of the major crystalline phases. At 2.0 mol% NiO fraction, this phase is replaced by $Li_3Zn_{0.5}SiO_4$. This occurs because of the change in the role of ZnO from network modifier to intermediate oxide as a result of NiO incorporation. The intermediate network forming Zn^{2+} ions would find it more difficult to diffuse and initiate the transformation of $Li_3Zn_{0.5}SiO_4$ to Li_2ZnSiO_4. The addition of NiO improves the performance of the glass–ceramic as a sealant to SS 321. Upon incorporation of 2% NiO, the glass–ceramic obtained displayed an interlocking, dendritic microstructure. The TEC of these materials was very closely matched with SS321, which we feel, will allow long service lives for these seals.

Acknowledgement The authors wish to thank Dr. Sinha and Dr. Purohit for providing XRD facility.

References

1. McMillan PW, Phillips SV, Partridge G (1966) J Mater Sci 1:269. doi:10.1007/BF00550175
2. Moddeman WE, Merten CW (1987) In: Kramer DP (ed) Technology of glass, ceramic or glass–ceramic to metal sealing. Amer. Soc. of Mech. Engineers, New York, p 31
3. Varshneya AK (1982) In: Tomozawa M, Doremus RH (eds) Treatise of materials science and technology, vol 22. Academic Press, New York, p 241
4. Donald IW, Metcalfe BL, Gerrard LA (2008) J Am Ceram Soc 91(3):715
5. Metcalfe BL, Donald IW, Bradley DJ (1991) In: Morrell R, Partridge G (eds) British ceramic society proceedings. Institute of Ceram, Stafford, p 177
6. Donald IW, Metcalfe BL, Morris AEP (1992) J Mater Sci 27:2979. doi:10.1007/BF01154109
7. Goswami M, Sengupta P, Sharma K, Kumar R, Shrikhande VK, Ferreira JMF, Kothiyal GP (2007) Ceram Int 33:863
8. Indrajit Sharma B, Goswami M, Sengupta P, Shrikhande VK, Kale GB, Kothiyal GP (2004) Mater Lett 58:2423
9. Yamane M, Mackenzie JD (1974) J Non-Cryst Solids 15(2):153
10. Arvind A, Sarkar A, Shrikhande VK, Tyagi AK, Kothiyal GP (2008) J Phys Chem Solids 69:2622
11. Chen Z-X, McMillan PW (1985) J Am Ceram Soc 68(4):220
12. Goel A, Shaaban ER, Ribeiro MJ, Melo FCL, Ferreira JMF (2007) J Phys Condens Matter 19:386231
13. Kingery WD (1963) Introduction to ceramics. Wiley, New York, p 145
14. Donald IW, Metcalfe BL, Wood DL, Copley JR (1989) J Mater Sci 24:3892. doi:10.1007/BF01168952
15. West AR, Glasser FP (1970) J Mater Sci 5:557. doi:10.1007/BF00554364
16. West AR, Glasser FP (1970) J Mater Sci 5:676. doi:10.1007/BF00549752
17. Donald IW (1993) J Mater Sci 28:2841. doi:10.1007/BF00354689